Bulletin of Electrical Engineering and Informatics
Vol. 15, No. 1, February 2026, pp. 373~383
ISSN: 2302-9285, DOI: 10.11591/eei.v15i1.10747

PULMO-NET: blockchain-integrated lung cancer classification using golden jackal optimization and GoogleNet

Angel Mary Azhakesan, Thanammal Kakkumperumal Krishnammal
Department of Computer Science, S.T. Hindu College (Affiliated to Manonmaniam Sundaranar University), Nagercoil, India

Article Info

Article history:

Received May 24, 2025
Revised Oct 10, 2025
Accepted Dec 6, 2025

Keywords:

Adaptive trilateral filter
Dragonfly algorithm
Golden jackal optimization
GoogleNet
Lung cancer

ABSTRACT

Lung cancer (LC) is a malignant disease caused by uncontrolled cell growth in the lungs, often associated with smoking and environmental factors. However, accurate LC classification is particularly challenging due to poor image quality, variability in imaging conditions, and noise artifacts in medical scans. In this work, a novel PULMO-NET is proposed for classifying LC using dual-modality imaging (CXR and CT). The dual-modality images are preprocessed using an adaptive trilateral (ADT) filter and segmented using the golden jackal optimization. The segmented lung regions are refined using the dragonfly algorithm (DA) which enables accurate extraction of diamond-shaped tumor patterns. Additionally, a blockchain-based system with local nodes is integrated to collect real-time patient data. GoogleNet uses inception modules to capture multi-scale features, enabling accurate classification of lung images into normal, non-small cell lung cancer (NSCLC), and small cell lung cancers (SCLC). The proposed PULMO-NET achieves the classification accuracy (AC) of 98.91% and F1 score of 96.51%. The PULMO-NET model improves the overall AC by 1.91%, 7.78%, and 4.33% better than Inception-v3, TPOT_SVM, and LeNet–DenseNet respectively.

Corresponding Author:

Angel Mary Azhakesan
Department of Computer Science, S.T. Hindu College (Affiliated to Manonmaniam Sundaranar University)
Nagercoil, Tamil Nadu, India
Email: anezkajoenirit21@gmail.com

1. INTRODUCTION

Lung cancer (LC) is the most common and fatal types of cancer globally [1], [2]. As the main cause of cancer-related fatalities, it becomes extremely deadly when found at an advanced stage [3]. This disease is caused by the formation of malignant tumors that start in the respiratory tract and usually spread rapidly [4], [5]. It affects millions of people each year and is common in both men and women [6]. According to 2024 statistics, 234,580 LC cases have been identified. 125,070 deaths from LC were recorded [7], [8]. LC is distinguished by uncontrolled cell proliferation, which affects normal pulmonary function and accelerates the disease [9]. LC is classified into two types like non-small cell lung cancer (NSCLC) and small cell lung cancers (SCLC). More than 85% of all cases of LC are NSCLC, making it the most common type [10]. However, these approaches are often costly, invasive, time-consuming, and prone to delays in early detection [11]. In recent years, computer-assisted diagnostics employing machine learning (ML) and deep learning (DL) has demonstrated encouraging findings for automating LC detection [12]. Optimization-based segmentation methods are limited by premature convergence, parameter sensitivity, high computational cost, and poor generalization across diverse clinical datasets [13].

Despite these advancements, several challenges remain. Existing computer-assisted approaches often suffer from high false-positive rates, difficulty in distinguishing between inter-class similarities and intra-class

variations, and poor performance when handling noisy or low-quality medical images [14]. Models struggle to accurately capture tumor features, leading to misclassification of nodules, and inadequate systems address secure handling of sensitive medical data in clinical practice [15]. This study looked into the effects of integrating adaptive trilateral (ADT) filtering, golden jackal optimization (GJO), dragonfly algorithm (DA), and blockchain-enabled secure classification for LC detection. While previous studies investigated the impact of DL and optimization methods for LC classification, they did not explicitly address their influence on handling noisy medical images, extracting fine-grained tumor features, and ensuring secure management of sensitive clinical data. To overcome these limitations, this research proposes a novel framework PULMO-NET, that integrates ADT filtering to improve image quality, GJO for precise lung segmentation, DA for robust tumor feature extraction, GoogleNet for accurate classification, and blockchain technology to ensure secure data management. The key contributions of this work are summarized as:

- The input images are collected from NIH CXR and LIDC-IDRI datasets, it providing comprehensive CXR and CT modalities for accurate LC detection and analysis.
- The dual input images are denoised by ADT filter to enhance image quality and eliminate the noisy distortions.
- The pre-processed images are input into GJO for lung region segmentation. That segmented images are divided into several cells, which are broken down into individual pixels.
- Each diamond-patterned cell has a center value and its surrounding bits selected using DA. Based on the center value, grayscale values were converted to binary values.
- Finally, these patterns are aggregated into the GoogleNet for classifying the images into tri classes such as SCLC, normal and NSCLC.

The structure of the paper is organized as follows, section 2 represents the literature survey, the PULMO-NET was explained in section 3, the performance outcomes and their comparison analysis were provided in section 4, and section 5 shows the discussion part. Section 6 encloses with conclusion.

Research hypothesis, the proposed approach raises the following scientific questions:

- SQ1: how can dual-modality imaging combined with ADT filter improve image quality and reduce noise artifacts for accurate LC classification?
- SQ2: what role does GJO play in enhancing lung region segmentation, and how does it compare with traditional segmentation methods?
- SQ3: how effectively does the DA capture fine-grained tumor patterns and contributes to robust feature extraction?

2. LITERATURE SURVEY

In recent years, the adoption of computer-assisted software in the medical field has gained significant attention due to the development of computerized methods for LC identification. A summary of some existing ML and DL models for LC detection and classification is presented in Table 1.

Table 1. Comparative analysis of existing LC detection and classification approaches

Author and year	Architecture	Dataset	Accuracy	Strengths	Weaknesses
Meeradevi *et al.* (2025) [16]	Multi-attribute decision-making	NIH CXR	97.05	Outperformed ML	Limited to CXR
Murthy and Thippeswamy (2025) [17]	TPOT+SVM	LIDC-IDRI CT	91.77	Automated optimization	High false positives
Mathew *et al.* (2025) [18]	Hybrid LeNet–DenseNet	LIDC-IDRI CT	94.8	High sensitivity	Lower specificity
Saha *et al.* (2025) [19]	Attention CNN+LGAM+federated learning	CT scans	91.5	Captures dependencies; includes XAI	Lower accuracy than SOTA
Eliwa *et al.* (2024) [20]	Blockchain+DenseNet	Lung and colon CT	92.34	Secure framework	Cloud dependency
Hosny et al. (2025) [21]	Hybrid Inception-ResNet	Multi-modal	97.65	Combines multiple imaging modalities	No single-modality benchmarking
Malik and Anees (2024) [22]	Multi-modal DL	Chest disease dataset	99.01	Very high accuracy	Dataset-specific, may not generalize

According to this survey, existing LC techniques suffer from high false positive rates, poor robustness to noisy images, difficulty in detecting small and overlapping nodules and inadequate mechanisms for secure medical data management. PULMO-NET addresses existing gaps by enhancing segmentation accuracy through GHAO, improving tumor feature extraction with the DA, and ensuring secure medical data management via blockchain integration.

3. PROPOSED PULMO-NET MODEL

In this research, a novel PULMO-NET is proposed for efficient classification of LC using dual input images. Figure 1 shows the proposed PULMO-NET methodology.

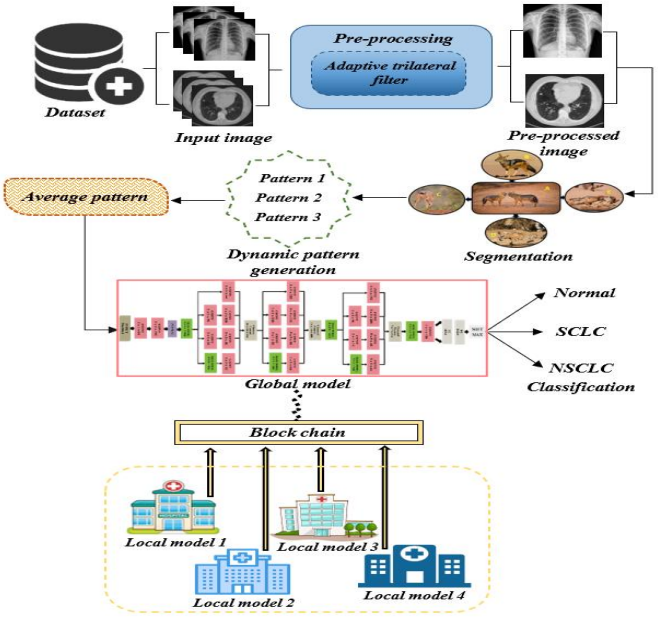

Figure 1. Proposed PULMO-NET methodology

3.1. Dataset description

The LIDC-IDRI dataset is used in this section to identify cases of LC. A total of 848 nodules, consisting of 406 malignant and 442 benign nodules, were recorded in the database, which has been expanded using 17 distinct methods. The NIH CXR database contains 112,120 CXR images, each of which corresponds to a distinct illness.

3.2. Data pre-processing

Dual-modality images are pre-processed using the ATF, which is based on the principles of a bilateral filter. Unlike the bilateral filter that struggles in high-gradient zones, ATF introduces a tilting mechanism to handle such regions effectively. The tilting angle of the trilateral filter is computed as (1):

$$h_\theta(q) = \frac{1}{l_\theta}\sum_q \sum_p f_p \, e(q,p) z(f_q, f_p) \quad (1)$$

The pixel value at the tilted plane is given by (2):

$$j(q,p) = f(q) + h_\theta.(||q-p||) \quad (2)$$

The final output after applying bilateral filtering and subtracting the local tilted plane is (3):

$$f_o(q) = f_{in}(y) + t(y)\Delta \quad (3)$$

where Δ is the spatial distance between pixels q and p, and $f_o(q)$ is the output function. ATF enhances image quality by smoothing noise while preserving high-gradient structures, thus overcoming the limitations of standard bilateral filtering.

3.3. Segmentation

The noise free images are fed into GJO to segment the lung region. GJO is an optimization method that derives inspiration from golden jackals' cooperative attacking style. Prey population (candidate solutions) is randomly initialized within given bounds. A fitness function evaluates each prey to determine solution quality.

The best two solutions are considered the male and female jackals, which guide the rest of the search. Jackals explore the search space by updating positions relative to male and female jackals. Positions are updated around the prey's location, leading to solution refinement and convergence. Through this cooperative hunting-inspired process, the jackals iteratively refine their positions until the lung region is effectively segmented.

3.4. Pattern generation

DA is an intelligent search-optimization method inspired by dragonflies' swarming behavior. It improves model efficiency and is an evolutionary algorithm. DA uses dynamic swarms to detect related features and enhance model efficiency. The distance between neighboring DFs is crucial for search space optimization and preventing collisions [23].

$$x_i = x_i + \Delta x_i \tag{4}$$

$$\Delta x_i = w\Delta x_i + (a.Sep_i + b.Alg_i + c.Coh_i + d.Af_i + e.Ee_i \tag{5}$$

where d stands for the food factor and e for the enemy component. The inertial weight is w, and the alignment, separation, and cohesion weights are a, b, and c. In this study, CT structural features in (1) and CXR statistical features in (2) were extracted using diamond-shaped kernels. These were then combined into a joint CT–CXR S2 fusion representation in (3) through a late-fusion strategy to capture complementary information. Patient-wise data splits were strictly maintained, and data balancing was applied to handle class distribution differences. This approach ensures that the fusion improves generalization while preventing data leakage.

Figure 2 illustrates the diamond pixel value patterns extracted from both imaging modalities. Figure 2(a) shows the pattern generation from a CXR image, while Figure 2(b) displays the corresponding pattern derived from a CT image. The patterns are generated by converting neighboring pixels' grayscale values into binary values. The altered bits are subjected to an XOR operation to obtain partial bits. This process can create three channels, such as 36 patterns with four bits per channel, with adjacent pixel values combining with the central pixel.

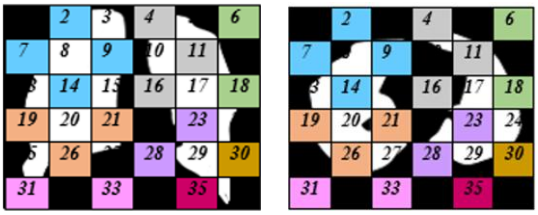

(a) (b)

Figure 2. Diamond pattern of pixel values; (a) CXR image and (b) CT image

3.5. Block chain

The PULMO-NET framework integrates blockchain [24] technology to secure medical imaging and classification data, ensuring data integrity, privacy, and tamper-proof storage. Each image is encrypted and hashed, generating a unique digital fingerprint. The framework supports real-time updates, secure access, and regulatory compliance. Although it introduces computational overhead, the benefits outweigh the overhead. It's scalable, suitable for multi-hospital and cloud-based deployments.

3.6. Global model

GoogleNet [25] also known as Inception-v1, uses Inception modules to efficiently classify input dual images into normal, SCLC, and NSCLC categories. These modules apply multiple convolutional filters simultaneously, enhancing the network's ability to handle information at different scales and record both fine and coarse features. GoogleNet is a convolutional process used for matching input data to multiple-size characteristics, particularly for recognizing structural damage.

3.7. Grad-CAM

Grad-CAM is a guided propagation technique that highlights critical regions in LC by feeding the gradient of a selected class into normal, SCLC, and NSCLC layers. It calculates the gradient c score and neuron significance weights.

$$t_h^g = \frac{1}{b} \sum r \sum sz \frac{\partial r^g}{\partial m^h} \tag{6}$$

Furthermore, a combination of feature maps is used to compute the Grad-CAM heatmap, which is subsequently followed by $relu$:

$$y_{Grad-CAM} = relu \sum_h f_h^g \, y^h \quad (7)$$

Grad-CAM calculates the gradient of neural layer influence in images, improving categorization precision and visual interpretability.

Figure 3 shows the flowchart of the proposed PULMO-NET for LC classification. To overcome the issues highlighted in the Introduction, the proposed methodology integrates ADT, GJAO, DA and GoogleNet with blockchain-enabled data security. These steps enhance image quality, enable precise feature extraction, and improve classification reliability, as validated by significant performance gains in LC detection.

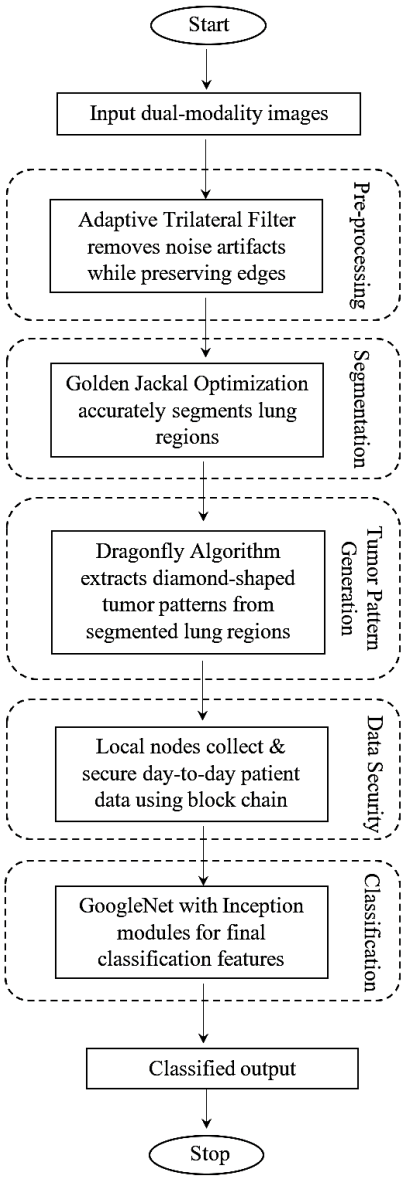

Figure 3. Flowchart of the proposed PULMO-NET for LC classification

4. RESULT

This section utilizes MATLAB-2019b, along with the DL toolbox to assess the effectiveness of the proposed model. Figure 4 displays the simulation results of the proposed PULMO-NET with dual image samples, including patient index, segmented images, diamond pattern, classification results, and abnormal lung images analyzed using Grad-CAM to highlight critical regions.

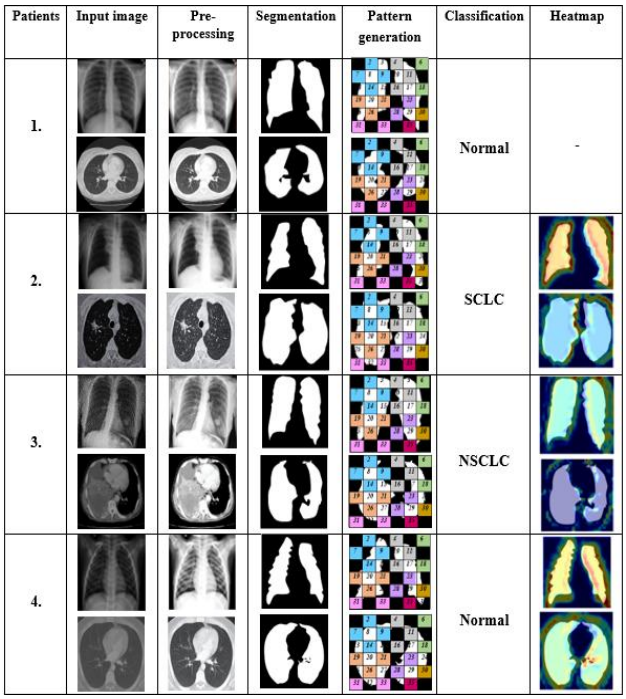

Figure 4. Experimental result of the proposed PULMO-NET

4.1. Performance analysis

A proposed PULMO-NET model was assessed based on, F1 score, specificity, recall, accuracy, and precision. Table 1 displays the classification performance attained by the proposed PULMO-NET model for LC. A total accuracy (AC) of 98.91% is achieved by the proposed PULMO-NET model using the dataset. The proposed PULMO-NET model also achieves 98.24%, 96.51%, 97.74%, and 97.48% overall precision (PR), F1 score (F1), specificity (SP), and recall (RE).

Table 1. Performance assessment of the proposed PULMO-NET model

Classes	AC	PR	RE	SP	F1
Normal	99.12	98.76	97.43	97.91	97.65
SCLC	98.36	97.13	98.14	96.75	96.14
NSCLC	99.25	98.83	96.87	98.58	95.76

Figure 5 shows the training and testing graph of proposed PULMO-NET model. The accuracy curve is shown in Figure 5(a), where accuracy and epochs are positioned on opposite axes. The model's accuracy rises as the number of epochs grows. As the number of epochs increases, the model's loss decreases, as seen by the epoch versus loss curve in Figure 5(b). The accuracy achieved by the suggested PULMO-NET model is 98.91%.

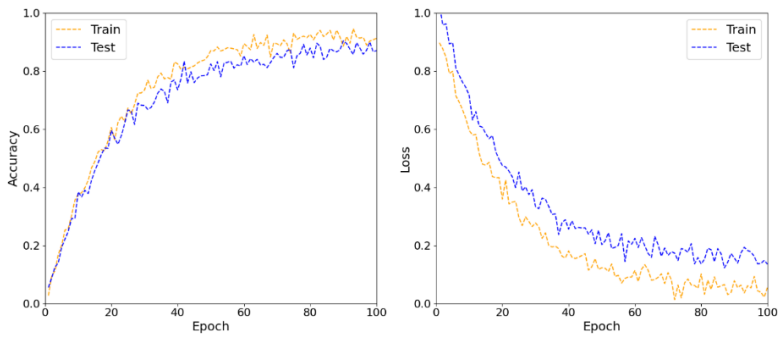

(a) (b)

Figure 5. Training and testing graph of the PULMO-NET model; (a) accuracy curve and (b) loss curve

Figure 6 presents the evaluation results of the proposed PULMO-NET model and the blockchain framework used in the system. Figure 6(a) shows that PULMO-NET achieves high accuracy, correctly classifying normal (0.99), SCLC (0.98), and NSCLC (0.99) with few misclassifications. Figure 6(b) presents the ROC curves, where all classes achieve AUC values above 0.98, the highest being 0.9913 for NSCLC. Figure 6(c) illustrates blockchain performance, showing that as hospital nodes increase, consensus latency rises from 150 ms to 800 ms and storage overhead grows from 5 MB to 22 MB, highlighting a trade-off between decentralization, delay, and storage cost.

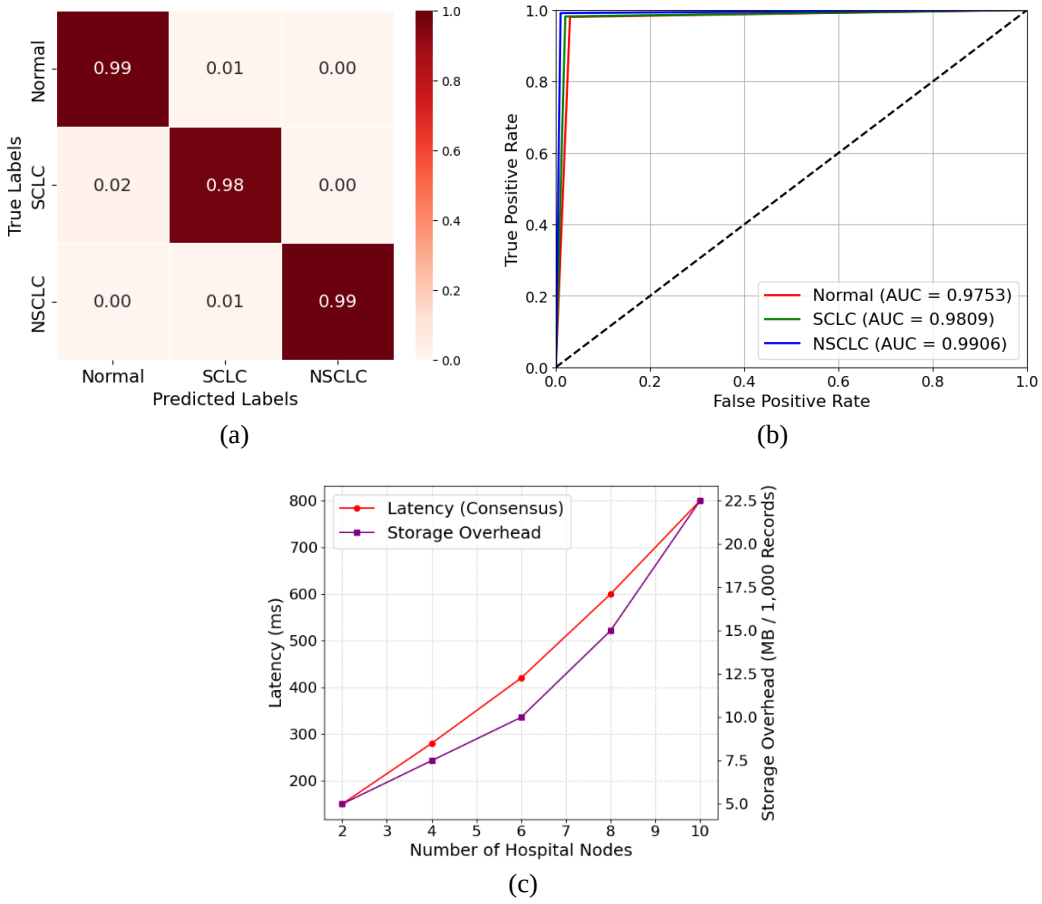

Figure 6. Overall performance of the proposed framework: (a) confusion matrix of PULMO-NET, (b) ROC curves with AUC scores for each class, and (c) blockchain performance in terms of latency and storage overhead

Table 2 displays PULMO-NET model cross-validation results using 3-fold and 5-fold methods on gathered datasets. The 3-fold method divides the dataset into three subsets, with 67% for training and 33% for testing, confirming the model's stability and high generalization ability.

Table 2. Cross-validation results of the proposed model

Metric	3-fold cross-validation (%)	5-fold cross-validation (%)
AC	98.53	98.70
F1	97.95	96.03
SP	96.80	95.86

4.2. Comparative analysis

The effectiveness of DL network was determined in order to validate that the suggested PULMO-NET generates results with a high level of AC. In Table 3, quantitative results demonstrate that the proposed GJO achieved the highest Dice index (DI) of 98.78% and IoU of 94.37% outperforming Graphcut, SegNet, and U-Net. These findings support the usefulness of the suggested technique for precision LC segmentation.

Table 3. Comparison of segmentation approaches

Methods	DI (%)	IoU (%)
Graphcut	92.79	89.27
SegNet	95.46	93.15
U-Net	97.21	91.84
GJO (ours)	98.78	94.37

Table 4 shows compare networks in terms of accuracy, p-value, average training time, inference time, GPU memory usage, and computational cost. The proposed PULMO-NET with GoogleNet achieves the highest accuracy of 98.91% with a significant p-value of 0.022, while maintaining efficient runtime of 14.2 s/epoch training, 7.1 ms/image inference, and moderate memory usage 3.5 GB. This balance ensures low computational cost and makes the model suitable for real-time clinical applications.

Table 4. Comparison of the PULMO-NET with existing models

Networks	Accuracy	p-value	Avg. training time (s/epoch)	Inference time (ms/image)	GPU memory usage (GB)	Computational cost
AlexNet	93.65	0.042	12.4	8.6	3.2	High
ShuffleNet	94.45	0.050	10.3	6.4	2.7	High
ConvNeXt	95.98	0.057	13.8	7.5	5.3	Moderate
MedSAM	96.37	0.040	17.5	10.3	5.9	Moderate
GoogleNet	98.91	0.022	14.2	7.1	3.5	Low

Our findings indicate that achieving higher accuracy of 98.91% in PULMO-NET is not associated with increased false positives, a common limitation reported in earlier works such as Inception-v3 of 97.05%, TPOT_SVM of 91.77%, and LeNet–DenseNet of 94.8%. The proposed method benefits from dual-modality imaging and advanced optimization without negatively affecting computational efficiency. We found that the proposed PULMO-NET framework achieved a strong correlation between improved image quality and accurate LC classification. The method attained an overall accuracy of 98.91%, with consistently higher PR, RE, and SP across all three classes of normal, SCLC, and NSCLC demonstrating a distinctly lower misclassification rate compared to existing approaches.

4.3. Ablation analysis

An ablation study of the PULMO-NET model for segmentation. The comparison of with GJO and without GJO. Table 5 shows that integrating ADT, GJO, DA, and blockchain significantly improves PULMO-NET's performance, achieving an AC of 98.91%, PR of 98.24%, SP of 97.74%, RE of 97.48%, and F1 of 96.51%. These results demonstrate that the combined components substantially enhance the model's reliability and overall effectiveness.

Table 5 shows that integrating ADT, GJO, DA, and blockchain significantly improves PULMO-NET performance, achieving an AC of 98.91%, RE of 97.48%, and F1 of 96.51%. These results demonstrate that the combined components substantially enhance the model's reliability and overall effectiveness.

Table 5. Performance comparison of the PULMO-NET with and without ADT, GJAO, DA, and blockchain

Metrics	With ADT, without GJO, DA, and blockchain	With GJO without ADT, DA, and blockchain	With DA without ADT, GJO, blockchain	With blockchain without ADT, GJO, and DA	With ADT, GJO, DA, and blockchain	Without ADT, GJO, DA, and blockchain
AC	92.91	93.10	95.64	90.12	98.91	93.87
RE	84.48	89.65	93.48	81.32	97.48	89.55
F1	93.16	86.32	92.51	89.83	96.51	90.28

4.4. Clinical settings

In this section, a clinical implication of the PULMO-NET was illustrated for efficiently classifying the LC. Figure 7 illustrates the workflow of LC classification using the proposed PULMO-NET. The process starts with the patient's hospital visit, where dual-modality images are collected for diagnosis. These images are processed by PULMO-NET, which analyzes them to predict the location and type of LC. The prediction outcomes assist doctors in refining diagnoses and planning appropriate treatments. This streamlined process enables real-time, accurate, and interpretable diagnoses while reducing diagnostic complexity. Moreover, PULMO-NET ensures seamless integration with healthcare systems, enhancing its practical applicability in clinical settings.

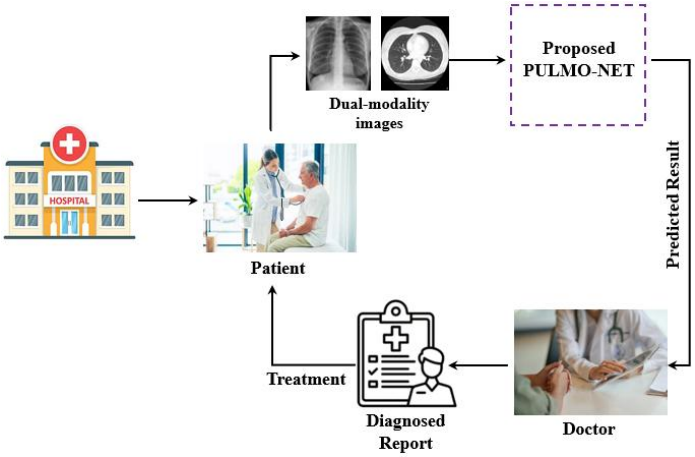

Figure 7. Real time clinical setting of the PULMO-NET

5. DISCUSSION

The PULMO-NET framework outperforms existing methods in lung segmentation and classification, with a Dice score of 98.78% and an IoU of 94.37%. Dual-modality approaches show better performance in practice, as CXR provides quick screening while CT offers detailed structural information. It uses ADT filtering, GJO, and DA for improved image quality and accuracy, enhancing reliability and generalization. In addition to improved accuracy, the integration of blockchain technology provides secure, immutable, and auditable management of classification results, addressing a critical limitation of most existing artificial intelligence (AI)-based diagnostic systems. This ensures that sensitive medical data are handled with trustworthiness, making the framework suitable for real clinical environments where both diagnostic accuracy and data security are essential. Our research shows that the PULMO-NET using dual-modality dataset, which may restrict its generalizability across other imaging modalities. Optimization-based segmentation methods are limited by premature convergence, parameter sensitivity, high computational cost, and poor generalization across diverse clinical datasets. Future research can focus on extending and validating PULMO-NET across additional modalities such as positron emission tomography (PET), magnetic resonance imaging (MRI), or histopathology images, and testing on larger, more diverse multi-institutional datasets to ensure robustness and real-time applicability in broader clinical settings.

6. CONCLUSION

This research introduces a novel PULMO-NET framework for LC classification using dual-modality images. PULMO-NET significantly enhances LC detection and classification, offering a robust tool for clinicians and radiologists. Recent observations indicate that traditional CNN-based models often suffer from noisy input and high false positives. Our findings offer clear evidence that the PULMO-NET framework overcomes these issues by integrating dual-modality imaging and optimization-based feature extraction, leading to more accurate and secure LC classification. For the research field, this study highlights the potential of combining blockchain technology with DL for secure, high-accuracy medical image analysis. The proposed GoogleNet improves its accuracy by 5.61%, 1.67%, 4.72%, and 8.60% better than AlexNet, DenseNet, ShuffleNet, and DarkNet. The proposed PULMO-NET model achieves the overall accuracy by 1.91%, 7.78%, and 4.33% comparing to the existing method such as Inception-v3, TPOT_SVM, and LeNet–DenseNet. The results demonstrate that the integration of dual-modality imaging, advanced feature extraction, and blockchain-based data management can significantly enhance LC classification performance. This advancement offers the research community and healthcare practitioners a more reliable, secure, and efficient framework for early detection and informed decision-making in LC management.

ACKNOWLEDGMENTS

The author would like to express his heartfelt gratitude to the supervisor for his guidance and unwavering support during this research for his guidance and support.

FUNDING INFORMATION

Authors state no funding involved.

AUTHOR CONTRIBUTIONS STATEMENT

This journal uses the Contributor Roles Taxonomy (CRediT) to recognize individual author contributions, reduce authorship disputes, and facilitate collaboration.

Name of Author	C	M	So	Va	Fo	I	R	D	O	E	Vi	Su	P	Fu
Angel Mary Azhakesan Thanammal Kakkumperumal Krishnammal	✓	✓	✓	✓	✓	✓	✓	✓	✓	✓	✓	✓	✓	

C : **C**onceptualization
M : **M**ethodology
So : **So**ftware
Va : **Va**lidation
Fo : **Fo**rmal analysis
I : **I**nvestigation
R : **R**esources
D : **D**ata Curation
O : Writing - **O**riginal Draft
E : Writing - Review & **E**diting
Vi : **Vi**sualization
Su : **Su**pervision
P : **P**roject administration
Fu : **Fu**nding acquisition

CONFLICT OF INTEREST STATEMENT

The authors declare that they have no known competing financial interests or personal relationships that could have appeared to influence the work reported in this paper.

INFORMED CONSENT

We certify that the nature and purpose of this study have been explained to the above-named individual, and the potential benefits of participating in this study have been discussed. All questions raised by the individual regarding the study have been answered, and the research team will remain available to address any future questions.

ETHICAL APPROVAL

This manuscript has been reviewed and ethically approved by our research guide for publication in this journal.

DATA AVAILABILITY

Data sharing not applicable to this article as no datasets were generated or analyzed during the current study.

REFERENCES

[1] L. D. L., K. Z. E., and S. D. K., "Pathological Anatomy and Differential Diagnosis of Small Cell Lung Cancer," in *International Conference on Modern Science and Scientific Studies*, 2025, pp. 84–89.
[2] S.-H. Xu, H. Xu, K.-W. Xiao, and S.-J. Mao, "Exercise rehabilitation on patients with non-small cell lung cancer: A meta-analysis of randomized controlled trials," *World Journal of Clinical Cases*, vol. 13, no. 11, Apr. 2025, doi: 10.12998/wjcc.v13.i11.100161.
[3] B. Ozdemir, E. Aslan, and I. Pacal, "Attention Enhanced InceptionNeXt-Based Hybrid Deep Learning Model for Lung Cancer Detection," *IEEE Access*, vol. 13, pp. 27050–27069, 2025, doi: 10.1109/ACCESS.2025.3539122.
[4] S. Zhu, D. Chen, X. Yang, L. Yang, and Y. Han, "Organoid Models to Study Human Infectious Diseases," *Cell Proliferation*, vol. 58, no. 11, Nov. 2025, doi: 10.1111/cpr.70004.
[5] N. Yuksel, B. Gelmez, and A. Yildiz-Pekoz, "Lung Microbiota: Its Relationship to Respiratory System Diseases and Approaches for Lung-Targeted Probiotic Bacteria Delivery," *Molecular Pharmaceutics*, vol. 20, no. 7, pp. 3320–3337, 2023, doi: 10.1021/acs.molpharmaceut.3c00323.
[6] C. E. Cotner and E. O'Donnell, "Understanding the Landscape of Multi-Cancer Detection Tests: The Current Data and Clinical Considerations," *Life*, vol. 14, no. 7, p. 896, Jul. 2024, doi: 10.3390/life14070896.
[7] Y. Katib and N. Mulla, "Epidemiological and clinical characteristics of lung cancer in Saudi Arabia: a retrospective study in single oncology center," *Oncology Research*, vol. 32, no. 11, pp. 1803–1809, 2024, doi: 10.32604/or.2024.052358.
[8] X. Li *et al.*, "Early detection of non-small cell lung cancer: an electronic health record data-driven approach," *BMC Medicine*, vol. 23, no. 1, p. 551, Oct. 2025, doi: 10.1186/s12916-025-04289-3.
[9] S. N. Kumar, A. Ahilan, A. L. Fred, and H. A. Kumar, "ROI extraction in CT lung images of COVID-19 using Fast Fuzzy C means clustering," in *Biomedical Engineering Tools for Management for Patients with COVID-19*, pp. 103–119, 2021, doi: 10.1016/B978-0-12-824473-9.00001-X.
[10] R. Nooreldeen and H. Bach, "Current and future development in lung cancer diagnosis," *International Journal of Molecular Sciences*, vol. 22, no. 16, p. 8661, Aug. 2021, doi: 10.3390/ijms22168661.

[11] J. Jayaram, S.-C. Haw, N. Palanichamy, S. K. Thillaigovindhan, and M. Al-Tarawneh, "Lung Tumor Segmentation in Medical Imaging Using U-NET," *Journal of Informatics and Web Engineering*, vol. 4, no. 1, pp. 140–151, Feb. 2025, doi: 10.33093/jiwe.2025.4.1.11.
[12] E. Bilgin, "Predicting Lung Cancer Severity Using Machine Learning Algorithms: Enhanced by Statistical Analysis," M.S. thesis, Dept. School of Computing, Montclair State University, New Jersey, USA, 2025.
[13] A. I. Dumachi and C. Buiu, "Applications of Machine Learning in Cancer Imaging: A Review of Diagnostic Methods for Six Major Cancer Types," *Electronics (Switzerland)*, vol. 13, no. 23, p. 4697, Nov. 2024, doi: 10.3390/electronics13234697.
[14] R. Abirami and P. Kumar, "Deep Learning Model for Accurate Brain Tumor Detection Using CT and MRI Imaging," *International Journal of System Design and Computing*, vol. 2, no. 01, pp. 26–31, 2024.
[15] S. L. Tan, G. Selvachandran, R. Paramesran, and W. Ding, "Lung Cancer Detection Systems Applied to Medical Images: A State-of-the-Art Survey," *Archives of Computational Methods in Engineering*, vol. 32, no. 1, pp. 343–380, Jan. 2025, doi: 10.1007/s11831-024-10141-3.
[16] T. Meeradevi, S. Sasikala, L. Murali, N. Manikandan, and K. Ramaswamy, "Lung cancer detection with machine learning classifiers with multi-attribute decision-making system and deep learning model," *Scientific Reports*, vol. 15, no. 1, p. 8565, Mar. 2025, doi: 10.1038/s41598-025-88188-w.
[17] N. N. Murthy and K. Thippeswamy, "TPOT with SVM hybrid machine learning model for lung cancer classification using CT image," *Biomedical Signal Processing and Control*, vol. 104, p. 107465, Jun. 2025, doi: 10.1016/j.bspc.2024.107465.
[18] A. Mathew, K. S. V. Grace, and M. M. S. J. Preetha, "An Approach for Lung Cancer Detection and Classification Using Lenet-Densenet," *Biomedical Engineering-Applications, Basis and Communications*, vol. 37, no. 1, Feb. 2025, doi: 10.4015/S1016237224500431.
[19] C. Saha *et al.*, "Lung-AttNet: An Attention Mechanism-Based CNN Architecture for Lung Cancer Detection with Federated Learning," *IEEE Access*, vol. 13, pp. 57369–57386, 2025, doi: 10.1109/ACCESS.2025.3554744.
[20] E. H. I. Eliwa, A. M. El Koshiry, T. Abd El-Hafeez, and A. Omar, "Secure and Transparent Lung and Colon Cancer Classification Using Blockchain and Microsoft Azure," *Advances in Respiratory Medicine*, vol. 92, no. 5, pp. 395–420, Oct. 2024, doi: 10.3390/arm92050037.
[21] M. Hosny, I. A. Elgendy, and M. A. Albashrawi, "Multi-Modal Deep Learning for Lung Cancer Detection Using Attention-Based Inception-ResNet," *IEEE Access*, vol. 13, pp. 123630–123648, 2025, doi: 10.1109/ACCESS.2025.3588407.
[22] H. Malik and T. Anees, "Multi-modal deep learning methods for classification of chest diseases using different medical imaging and cough sounds," *PLoS ONE*, vol. 19, no. 3, p. e0296352, Mar. 2024, doi: 10.1371/journal.pone.0296352.
[23] M. A. S. I. Tinu, A. Appathurai, and N. Muthukumaran, "Detection of Brain Tumour Via Reversing Hexagonal Feature Pattern for Classifying Double-Modal Brain Images," *IETE Journal of Research*, vol. 70, no. 8, pp. 7033–7043, Aug. 2024, doi: 10.1080/03772063.2023.2301663.
[24] V. K. Ravindran, "Quick-Chain: Blockchain Enabled Secure Data Transmission in Iot-Wsn Environment," *International Journal of Computer and Engineering Optimization*, vol. 2, no. 02, pp. 35-39, 2024.
[25] R. Pandian, V. Vedanarayanan, D. N. S. R. Kumar, and R. Rajakumar, "Detection and classification of lung cancer using CNN and Google net," *Measurement: Sensors*, vol. 24, p. 100588, Dec. 2022, doi: 10.1016/j.measen.2022.100588.

BIOGRAPHIES OF AUTHORS

Angel Mary Azhakesan is currently a research scholar in the Department of Computer Science and Research Centre at S.T. Hindu College, Nagercoil affiliated with Manonmaniam Sundaranar University Tirunelveli, Tamil Nadu, and is pursuing her research under the esteemed Manonmaniam Sundaranar University. She can be contacted at email: anezkajoenirit21@gmail.com.

Thanammal Kakkumperumal Krishnammal received the M.Sc. (Computer Science) degree from Bharathidasan University, Tiruchirappalli, in 1992, the M.Phil. (Computer Science) degree from Manonmaniam Sundaranar University, Tirunelveli, in 1999, the M.Tech. (Computer Science) degree from Vinayaka Mission University, Salem, in 2007, and the Ph.D. (Computer Science) degree from Manonmaniam Sundaranar University, Tirunelveli, in 2015. She can be contacted at email: kktcs@sthinducollege.com.